Published in final edited form as:
Toxicol Sci. 2008 May ; 103(1): 35–45. doi:10.1093/toxsci/kfn038.

Characterization of Organic Anion Transporting Polypeptide 1b2-null Mice: Essential Role in Hepatic Uptake/Toxicity of Phalloidin and Microcystin-LR

Hong Lu[*], **Supratim Choudhuri**[†], **Kenichiro Ogura**[‡], **Iván L. Csanaky**[*], **Xiaohong Lei**[*], **Xingguo Cheng**[*], **Pei-zhen Song**[*], and **Curtis D. Klaassen**[*,1]

[*]Department of Pharmacology, Toxicology and Therapeutics, University of Kansas Medical Center, Kansas City, Kansas [†]Center for Food Safety and Nutrition, Food and Drug Administration, College Park, Maryland [‡]Department of Drug Metabolism and Molecular Toxicology, Tokyo University of Pharmacy and Life Science, Tokyo, Japan

Abstract

The liver-specific importer organic anion transporting polypeptide 1b2 (Oatp1b2, Slco1b2, also known as Oatp4 and Lst-1) and its human orthologs OATP1B1/1B3 transport a large variety of chemicals. Oatp1b2-null mice were engineered by homologous recombination and their phenotype was characterized. Oatp1b2 protein was absent in livers of Oatp1b2-null mice. Oatp1b2-null mice develop normally and breed well. However, adult Oatp1b2-null mice had moderate conjugated hyperbilirubinemia. Compared with wild-types, Oatp1b2-null mice had similar hepatic messenger RNA expression of most transporters examined except a higher Oatp1a4 but lower organic anion transporter 2. Intra-arterial injection of the mushroom toxin phalloidin (an Oatp1b2-specific substrate identified *in vitro*) caused cholestasis in wild-type mice but not in Oatp1b2-null mice. Hepatic uptake of fluorescence-labeled phalloidin was absent in Oatp1b2-null mice. Three hours after administration of microcystin-LR (a blue-green algae toxin), the binding of microcystin-LR to hepatic protein phosphatase 1/2a was much lower in Oatp1b2-null mice compared with wild-type mice. In contrast, Oatp1b2-null mice were transiently protected from decrease in bile flow induced by estradiol-17β-D-glucuronide, a common substrate for Oatps. Oatp1b2-null mice were completely resistant to the hepatotoxicity induced by phalloidin and microcystin-LR, but were similarly sensitive to α-amanitin–induced hepatotoxicity compared with wild-type mice. In conclusion, Oatp1b2-null mice display altered basic physiology and markedly decreased hepatic uptake/toxicity of phalloidin and microcystin-LR. Oatp1b2-null mice are useful in elucidating the role of Oatp1b2 and its human orthologs OATP1B1/1B3 in hepatic uptake and systemic disposition of toxic chemicals and therapeutic drugs.

Keywords

Oatp1b2; liver; knockout; mice; phalloidin; microcystin

[1]To whom correspondence should be addressed at Department of Pharmacology, Toxicology and Therapeutics, University of Kansas Medical Center, 3901 Rainbow Blvd., Kansas City, KS 66160-7417. Fax: (913) 588-7501. cklaasse@kumc.edu. .
Hong Lu, Supratim Choudhuri, and Kenichiro Ogura contributed equally to this study.

Many transporters are responsible for uptake of endogenous and exogenous chemicals into liver, including the organic anion transporting polypeptides (Oatps), Na^+-taurocholate-cotransporting polypeptide (Ntcp), organic anion transporters (Oats), and organic cation transporters (Klaassen and Lu, 2007). Among these transporters, the Oatps are thought to be responsible for the majority of hepatic uptake of chemicals, whereas Ntcp mainly transports bile acids into liver (Trauner and Boyer, 2003). Oats and organic cation transporters are predominantly expressed in kidney and are thought to be less important in liver. Though the name Oatp implies selective transport of organic anions, certain Oatps can also transport organic cations and neutral compounds (Hagenbuch and Meier, 2004; Konig *et al*., 2006). Rodent Oatp1a1, 1a4, 1b2, and 2b1, as well as human OATP1B1, 1B3, and 2B1 are highly expressed in liver (Cheng *et al*., 2005; Choudhuri *et al*., 2000; Hagenbuch *et al*., 2000; Li *et al*., 2002; Ogura *et al*., 2000). The mouse/rat liver-specific importer Oatp1b2 (also known as Oatp4, Lst-1, gene symbol Slco1b2), first cloned in our laboratory (Choudhuri *et al*., 2000; Ogura *et al*., 2000), is orthologous to human OATP1B1 (also known as OATP-2) and OATP1B3 (also known as OATP-8) (Hagenbuch and Meier, 2003).

The organic anionic dye dibromosulfophthalein (DBSP) disulfonate is rapidly extracted from the circulation by hepatocytes, and is almost entirely eliminated in bile. Thus, clearance of DBSP is used to determine liver function (Dhumeaux *et al*., 1974). The nonmetabolizable feature of DBSP makes it an excellent chemical to characterize the pure role of transporters in hepatic uptake and biliary excretion of chemicals.

Certain chemicals selectively accumulate in liver to produce hepatotoxicity, such as the mushroom toxins phalloidin and amanitin (in *Amanita phalloides*) as well as the blue-green algae toxin microcystin-LR. It was proposed that these toxic cyclic peptides are transported into hepatocytes by the same multispecific transport systems that mediate hepatic uptake of bile acids (Eriksson *et al*., 1990; Kroncke *et al*., 1986). However, recent cellular studies showed that rat Oatp1b2 as well as human OATP1B1 and OATP1B3, but not other Oatps (Oatp1a1, Oatp1a4, OATP2B1) or Ntcp, transport phalloidin (Meier-Abt *et al*., 2004) and microcystin-LR (Fischer *et al*., 2005), whereas rat Ntcp and human OATP1B3 may mediate hepatic uptake of α-amanitin (Gundala *et al*., 2004; Letschert *et al*., 2006). Accidental ingestion of *Amanita phalloides* and environmental pollution of microcystin are important clinical causes of liver injury (Bischoff, 2001; Faulstich and Wieland, 1996). The *in vivo* importance of Oatp1b2 and OATP1B1/1B3 in mediating the hepatic uptake and toxicity of these three toxins remains to be elucidated.

Intrahepatic cholestasis of pregnancy (ICP) is a benign disease for the mother but associated with an increased perinatal morbidity and mortality. Hypersensitivity to elevated estrogens, particularly estrogen glucuronide, is implicated as a major cause of ICP (Fagan, 1999). In rodents, estradiol-17β-D-glucuronide ($E_2$17βG), the major estrogen glucuronide *in vivo*, induces an immediate, profound, but reversible inhibition of bile flow (Meyers *et al*., 1980). Many of the functionally characterized Oatps are able to transport $E_2$17βG *in vitro* (Hagenbuch and Meier, 2003); thus, the importance of a single Oatp, namely Oatp1b2 herein, in mediating $E_2$17βG-induced cholestasis remains to be determined.

In humans, functional polymorphisms of OATP1B1 (with decreased uptake activity) are associated with elevated blood levels of a number of therapeutic drugs, such as the cholesterol-lowering drugs statins (pravastatin, pitavastatin, and simvastatin) (Ho *et al*., 2007; Ieiri *et al*., 2007; Pasanen *et al*., 2006), the antidiabetic drugs nateglinide and repaglinide (Niemi *et al*., 2005a; Zhang *et al*., 2006), as well as the H_1-receptor antagonist fexofenadine (Niemi *et al*., 2005b).

We hypothesize that Oatp1b2 has an important and unique role in hepatic uptake of chemicals, and that the loss of its function cannot be compensated by other hepatic importers. We engineered Oatp1b2-null mice by homologous recombination and characterized their phenotype. Oatp1b2-null mice develop normally and breed well. However, Oatp1b2-null mice have changes in blood chemistry. To characterize the role of Oatp1b2 in hepatic uptake and systemic disposition of chemicals, we investigated the pharmacokinetics and/or hepatotoxicity of five chemicals, namely DBSP (a nonmetabolizable xenobiotic), phalloidin and microcystin-LR (*in vitro* specific substrates for Oatp1b2), α-amanitin, and $E_2$17βG (a common endogenous substrate for Oatps).

MATERIALS AND METHODS

Chemicals and reagents

Phalloidin, fluorescein isothiocyanate–labeled phalloidin (phalloidin-FITC, P5282), α-amanitin, microcystin-LR, and $E_2$17βG were purchased from Sigma, Inc. (St Louis, MO). DBSP was acquired from SERB Laboratories (Paris, France). Analytical kits for total and direct bilirubin, bile acids, alanine transaminase (ALT), alkaline phosphatase (ALP), and urea nitrogen were obtained from Wako Chemicals USA, Inc. (Richmond, VA) and Pointe Scientific Inc. (Canton, MI), respectively.

Development of Oatp1b2-null mouse

The mouse *Oatp1b2* cDNA and gene were cloned and characterized in our laboratory (Ogura *et al*., 2000). The targeting vector for the disruption of *Oatp1b2* gene was created by cloning part of the mouse *Oatp1b2* gene (intron 1 through part of intron 3) into the pKO scrambler NTKV-1902 (Stratagene, La Jolla, CA).

The 5′ fragment of the targeting construct was generated and subcloned as two separate fragments: 5′ fragment no. 1 (more upstream of the two) and 5′ fragment no. 2 (more downstream of the two). The 5′ fragment #1 was PCR-amplified as a ~1.08-kb *Hin*dIII–*Hin*dIII fragment which included sequences spanning from intron 1 through exon 2. The 5′ fragment no. 2 was generated as a *Hin*dIII–*Cla*I fragment, and was first subcloned into pBluescript. PCR primers were designed to introduce *Cla*I and *Bam*HI sites, and the 5′ fragment no. 2 was amplified as a ~1.3-kb *Hin*dIII–*Cla*I fragment, which included sequences spanning from exon 2 through part of exon 3. The longer 3′ fragment of the targeting construct was generated as a *Bam*HI–*Kpn*I fragment. The final nonlinearized targeting vector (Fig. 1A) had a neo-gene cassette that was flanked by a short arm (*Hin*dIII–*Cla*I; ~2.4-kb, containing intron 1 through part of exon 3) and a long arm (*Bam*HI–*Kpn*I; ~6 kb, containing the rest of exon 3 and part of intron 3) of the mouse *Oatp1b2* gene.

Upon *Not*I linearization, the linearized targeting vector was about 14-kb long; it contained the long arm (~7.4 kb) that included the *neo* cassette, short arm (~2.4 kb), and ~3.8-kb vector-derived sequence, which included the thymidine kinase (*TK*) gene sequence. The nucleotide (nt) positions of the major segments in the final targeting vector are as follows: Myeloid Cells-1 promoter: 12–300; TK: 377–1507; TK polyA: 1523–2019; Mouse *Oatp1b2* gene 5′-end (intron 1 through part of exon 3): 2068–4489; loxP: 4490–4524; bgh polyA-Neomycin phosphotransferase (neo)-phosphoglycerate kinase promotor: 4552–6155; loxP: 6171–6205; Mouse *Oatp1b2* gene 3′-end (the rest of exon 3 and part of intron 3): 6214–9902 (this region contains about 3.5-kb unsequenced part of intron 3 and also an *Acc*I site); *Not*I site: 9945. Figure 1B (upper panel) shows the targeting strategy through homologous recombination.

The *Not*I-linearized targeting vector was electroporated into W9.5 ES cell line (129S1). Upon selection with 300 mg/ml G418 and 2mM gancyclovir, 216 individual ES cell clones

were isolated for Southern blot analysis. Three clones were identified as homologously recombined clones by 5′ external, 3′ external, and *neo* probes. These three clones were further karyotyped to confirm that no chromosomal aberration occurred upon targeting. Two of these clones were confirmed to have 100% wild-type karyotype. Both clones were used for blastocyst injection by Xenogen Biosciences (Cranbury, NJ). From one of these clones, 10 male chimeras were produced and two of the 100% male chimeras were used for breeding (C57BL/6). Heterozygous F1 mice were produced from both chimeras. Interbreeding of heterozygous F1 mice produced homozygous F2 mice of both sexes in a mixed genetic background of C57BL/6 and 129Sv. Oatp1b2-null mice were then backcrossed to C57BL/6 background for six generations. PCR primers used for genotyping *Oatp1b2*-null mice are: KO-A: 5′-TGGCTTCTGAGGCGGAAAGA-3′; COMA: 5′-ATGGTTGGGGTTGACATCTCG-3′; WT-A: 5′-TCCATCGCAGTGCCTTGTCTT-3′. The *Oatp1b2*-null mice produced a single band of 261 bp, whereas the wild-type mice produced a single band of 225 bp after gel electrophoresis of the PCR products of tail DNA (Fig. 1B; lower panel, left). Consistent with the result of targeting, no Oatp1b2 protein could be detected in *Oatp1b2*-null mice as revealed by the Western blot (Fig. 1B; lower panel, right). PCR genotyping protocol is available upon request.

Treatment of animals

Mice were maintained at an American Animal Associations Laboratory Animal Care-accredited facility at the University of Kansas Medical Center (KUMC). Age-matched C57BL/6 and 129Sv mice were purchased from Charles River Laboratories, Inc. (Wilmington, MA) and allowed at least one week to adapt to the environment before being used for the experiments. Mice were housed at an ambient temperature of 22 °C with alternating 12-h light/dark cycles, and allowed water and rodent chow *ad libitum* (Teklad 8604; Harlan, Indianapolis, IN). All animal procedures in this study were approved by the Institutional Animal Care and Use Committee of KUMC.

In the initial studies on the toxicity of mushroom toxins, phalloidin, and α-amanitin, adult male Oatp1b2-null mice in the mixed genetic background were used; age-matched male C57BL/6 and 129Sv mice were used as wild-type controls. The dosages of phalloidin and α-amanitin were selected based on literature and pilot experiments. Mice were injected ip with phalloidin (2.5 mg/kg in saline) or saline (10 ml/kg). Blood and liver samples were collected 6-h postinjection under pentobarbital anesthesia. Liver samples were fixed in 10% neutral formalin, processed by standard histopathological techniques, and liver sections (5 μm) stained with hematoxylin–eosin were examined under light microscopy. In a second study, mice were injected ip with α-amanitin (1.0 mg/kg in saline) or saline (10 ml/kg), and blood and liver samples were collected 16 h later under pentobarbital anesthesia. In all the other experiments, Oatp1b2-null mice backcrossed to C57BL/6 mice for six generations were used, and age-matched C57BL/6 mice were used as wild-type controls.

In the study of blood chemistry (Table 1) and hepatic expression of transporters, blood samples of adult (3 months old) male and female Oatp1b2-null and C57BL/6 mice were drawn from the carotid artery via a cannula under anesthesia. Mouse serum samples (0.5 ml) were analyzed by Physicians Reference Laboratory (Overland Park, KS). Mouse tissue samples were collected and weighed. Liver samples were used for preparation of total RNA and protein samples.

In the study of microcystin-LR–induced hepatotoxicity, male adult Oatp1b2-null and C57BL/6 mice were injected ip with microcystin-LR (120 μg/kg in saline) or saline (10 ml/kg). Mouse blood and liver samples were collected 20-h postinjection under pentobarbital anesthesia.

Biliary excretion and pharmacokinetic study

Mice were anesthetized by ip injection of ketamine (100 mg/kg)–midazolam (5 mg/kg), and their body temperatures were maintained at 37 °C by means of heating pads. Subsequently, the right carotid artery was cannulated with PE-10 tubing, and the common bile duct was cannulated with the shaft of a 30-gauge needle attached to PE-10 tubing. Bile samples were collected in 15-min periods into preweighed tubes for five periods (15 min prior to until 60 min after injection). After the first bile-collecting period, the test chemical was injected into the carotid cannula, and 25–30 μl of blood were taken at 2-, 7.5-, 22.5-, 37.5-, and 52.5-min postinjection into heparinized tubes. The volumes of bile samples were measured gravimetrically with 1.0 used as the specific gravity of bile. One-hour postinjection, the livers were harvested.

DBSP (120 μmol/kg) was dissolved in pathogen-free water and injected at 10 ml/kg. Plasma and bile samples were alkalized by being admixed with an equal volume of 0.1*N* NaOH, and DBSP concentrations were quantified spectrophotometrically (Gregus and Klaassen, 1982). A NanoDrop ND-1000 spectrophotometer (NanoDrop Technologies, Wilmington, DE), which only requires 1 μl of sample for measurement, allowed an accurate quantification of plasma levels of DBSP.

For the study of phalloidin-induced cholestasis, adult male Oatp1b2-null and C57BL/6 mice were injected intra-arterially with phalloidin 0.4 mg/kg (0.32 mg/kg phalloidin + 0.08 mg/kg phalloidin-FITC). One h after phalloidin injection, livers were harvested and slices of liver samples were frozen on dry ice and stored at −80 °C for detection of phalloidin-FITC in mouse liver. For the study of $E_2$17βG-induced decrease in bile flow, adult female Oatp1b2-null and C57BL/6 mice were injected intra-arterially with $E_2$17βG (24 μmol/kg in 10 ml/kg of 0.02*N* NaOH).

Detection of phalloidin-FITC in mouse liver

Frozen liver sections (5 μm) were fixed with 4% paraformaldehyde for 5 min and washed with phosphate buffered saline containing 0.1% Triton X-100. Sections were air dried and mounted in Prolong Gold with 4′,6-diamidino-2-phenylindole (DAPI, nuclear stain) (Invitrogen Corp., Carlsbad, CA). Images were captured on an Olympus BX41 fluorescent microscope with a DP70 camera and DP Controller software. Each fluorescent channel (for FITC and DAPI staining) was acquired sequentially and then merged to create the final image. Images were cropped and brightness and contrast were adjusted under uniform conditions in Adobe Photoshop CS2 (San Jose, CA).

Development of peptide specific antibodies to detect mouse Oatp1b2 protein

A 25 amino acid long peptide epitope specific for mouse Oatp1b2 (protein_id NP_065241), CNPEPVNNNGYSCVPSDEKNSETPL (666–689) was designed using DS Gene software (Accelrys Inc., San Diego, CA). This peptide epitope was synthesized and conjugated with maleimide-activated keyhole limpet hemocyanin and used to produce affinity-purified rabbit polyclonal antibodies (Bethyl Laboratories, Montgomery, TX).

Western blot analysis of Oatp1b2 protein

Protein expression of Oatp1b2 in crude membrane fractions prepared from livers of wild-type and Oatp1b2-null mice was determined by Western blot (Chen *et al*., 2005). Protein concentrations were determined with Bradford reagent. Briefly, protein samples (50 μg) were loaded onto 10% sodium dodecyl sulfate polyacrylamide gel electrophoresis (SDS–PAGE) gels. After electrophoresis, proteins were transferred to polyvinylidene fluoride membranes, and filters were probed with a polyclonal antibody against mouse Oatp1b2.

Signals were visualized with horseradish peroxidase–conjugated secondary antibody (Amersham Biosciences, Piscataway, NJ).

Western blot detection of microcystin-LR in nuclear or cytosolic extracts

Adult male C57BL/6 and Oatp1b2-null mice were injected ip with microcystin-LR (60 μg/kg) and livers were removed 3 h after microcystin administration. Livers were homogenized in a buffer (25mM 4-(2-hydroxyethyl)-1-piperazineethanesulfonic acid, pH 7.6, 1.5mM ethylenediaminetetraacetic acid, 10% glycerol, 1mM dithiotreitol, 0.1 mg/ml phenylmethylsulfonyl fluoride, 0.5M KCl, and 1× protease inhibitor cocktail). After being incubated on ice for 1 h, the homogenates were centrifuged at 100,000 × g for 30 min at 4 °C. The resultant supernatant was stored at −80 °C. Protein concentrations were determined with Bradford reagent. A total of 20 μg of protein from nuclear or cytosolic extracts were boiled for 2 min and loaded to 10% SDS–PAGE gels. After electrophoresis, proteins were transferred to polyvinylidene fluoride membranes and filters probed with a primary anti-microcystin monoclonal antibody (Mouse IgG1, clone MC10E7, AXXORA, LLC, San Diego, CA). Signals were visualized with horseradish peroxidase–conjugated secondary antibody.

RNA extraction

Total tissue RNA was extracted using RNA-Bee reagent (Tel-Test, Inc., Friendswood, TX) according to the manufacturer's protocol. Each RNA pellet was redissolved in 0.2 ml of diethyl pyrocarbonate-treated water. RNA concentrations were quantified by ultraviolet absorbance at 260 nm.

Branched DNA signal amplification assay

The branched DNA (bDNA) assay is a high-throughput and quantitative method for messenger RNA (mRNA) quantification (Canales *et al*., 2006), which has been used extensively in our laboratory. The mRNA of genes examined was quantified using Quantigene bDNA signal amplification kit (Panomics, Fremont, CA) with modifications (Leazer and Klaassen, 2003). The probes for all mouse genes determined herein have been reported previously (Buist and Klaassen, 2004; Cheng *et al*., 2005; Maher *et al*., 2005). Luminescence of the 96-well plate was quantified with a Synergy 2 Microplate reader (BioTek Instruments, Inc., Winooski, VT). The luminescence for each well is reported as relative light units (RLU) per 10 μg of total RNA.

Statistics

Data are presented as mean ± standard error. Differences between groups were determined by ANOVA, followed by Duncan's multiple-range test with significance set at $p < 0.05$.

RESULTS

Hepatic Expression of Major Uptake and Efflux Transporters in Oatp1b2-null Mice

To investigate whether knockout of Oatp1b2 causes compensatory alterations in hepatic expression of other transporters, we quantified hepatic mRNA expression of major uptake and efflux transporters. There is no gender difference in hepatic mRNA expression of Oatp1b2 in wild-type mice (Fig. 2). In Oatp1b2-null mice, the truncated Oatp1b2 mRNA was detected, but with much lower RLUs compared with wild-type mice. Hepatic mRNA expression of most transporters remained unchanged, namely Oatp1a1 (also known as Oatp1), Oatp2b1, Ntcp, bile salt export pump, adenosine triphosphate binding cassette g5/g8, multidrug resistance protein 2, multidrug resistance–associated protein 2 (Mrp2), Mrp4, Mrp5, Mrp6, and breast cancer resistance protein (data not shown). However, compared

with wild-type mice, male and female Oatp1b2-null mice had 2.5- and 1.1-fold higher hepatic mRNA expression of Oatp1a4 (also known as Oatp2) but 50 and 43% lower mRNA expression of Oat2, respectively (Fig. 2). Wild-type female mice had higher hepatic mRNA expression of Mrp3 than wild-type males. Oatp1b2-null males had 97% higher hepatic Mrp3 mRNA than wild-type males, in contrast to similar hepatic levels of Mrp3 transcripts in both genotypes of female mice (Fig. 2).

Alteration in Blood Chemistry in Oatp1b2-null Mice

Oatp1b2-null mice develop and breed well, and the relative liver/body weight ratio remained unchanged in both genders of Oatp1b2-null mice (data not shown). The blood chemistry of Oatp1b2-null mice remained generally normal with a few exceptions. Blood levels of glucose, urea nitrogen, creatinine, globulin, ALP, aspartate aminotransferase, lipase, creatine phosphokinase, calcium, phosphorus, potassium, and CO_2 remained similar between wild-type and Oatp1b2-null mice (data not shown). In Oatp1b2-null females, the most notable finding was a 2.5-fold elevation in serum levels of total bilirubin, which was almost entirely due to an increase in conjugated bilirubin. In contrast, in Oatp1b2-null males, serum levels of unconjugated bilirubin tended to be higher ($p = 0.067$), compared with wild-type males. A change observed in Oatp1b2-null males was a 30% increase in serum levels of total cholesterol compared with wild-type males. In both genders of Oatp1b2-null mice, serum levels of total protein and albumin increased slightly. Additionally, slight but statistically significant changes in blood chemistry were detected in Oatp1b2-null females, including increased serum levels of ALT, sodium, and chloride, as well as decreased serum levels of amylase compared with wild-type females.

Plasma Levels and Biliary Excretion of DBSP in Oatp1b2-null Mice

After intra-arterial injection, plasma levels of DBSP decreased rapidly in wild-type mice but much slower in Oatp1b2-null mice (Fig. 3A). Consequently, plasma levels of DBSP remained 4.8-fold higher in Oatp1b2-null compared with wild-type mice at 52.5 min after DBSP administration. The area under curve of blood levels of DBSP is 4950 and 14,900 μmol/min/l in wild-type and Oatp1b2-null mice, respectively. DBSP did not alter bile flow in either genotype of mice (Fig. 3B). The biliary excretion of DBSP in wild-type mice was rapid: within 1 h after injection, more than 95% of the administered DBSP was excreted into bile. The initial biliary excretion of DBSP for the first and second 15-min collection period was 48% and 33% less in the Oatp1b2-null mice (Fig. 3C), and the 1-h cumulative biliary excretion of DBSP was 30% less (Fig. 3D) in Oatp1b2-null compared with wild-type mice.

Role of Oatp1b2 in Mediating the Decrease in Bile Flow Induced by $E_2$17βG

$E_2$17βG, a common substrate for Oatp1a1, 1a4, and 1b2, was used to investigate the role of Oatp1b2 in hepatic uptake of common substrates for Oatps. There was no difference in the basal rate of bile flow between female wild-type and Oatp1b2-null mice (Fig. 4). Intra-arterial injection of $E_2$17βG into wild-type female mice induced a 78% decrease in bile flow 30-min postinjection (Fig. 4). The initial decrease in bile flow induced by $E_2$17βG was attenuated in Oatp1b2-null females; however, such protection faded gradually, resulting in similar bile flow between wild-type and Oatp1b2-null females 1 h after $E_2$17βG administration.

Role of Oatp1b2 in Mediating Hepatic Uptake of Phalloidin and Phalloidin-Induced Cholestasis

Similar to females, there was no difference in the basal rate of bile flow between male wild-type and Oatp1b2-null mice (Fig. 5A). Wild-type mice had severe cholestasis 1 h after intra-arterial injection of phalloidin 400 μg/kg (containing 80 μg/kg phalloidin-FITC) (Fig. 5A).

This phalloidin-induced decrease in bile flow was substantially attenuated in Oatp1b2-null males throughout the entire experimental period. One h after phalloidin administration, the rates of bile flow were 7 and 53% of the initial values in wild-type and Oatp1b2-null males, respectively. One-hour postinjection, phalloidin-FITC was associated with the inner plasma membrane of all hepatocytes of wild-type mice (Fig. 5B), but was absent in hepatocytes of Oatp1b2-null mice (Fig. 5C, indicating a lack of hepatic uptake of phalloidin in Oatp1b2-null mice.

Differential Roles of Oatp1b2 in Mediating Hepatotoxicity of Mushroom Toxins

Phalloidin induces a rapid disruption of hepatocytes. Serum levels of ALT were highly elevated in both strains of wild-type mice (Fig. 6A) 6 h after ip injection of phalloidin (2.5 mg/kg). By gross examination, the livers of phalloidin-treated wild-type mice were swollen and markedly hemorrhagic. Oatp1b2-null mice (in a mixed genetic background of C57BL/6 and 129Sv) were completely protected from phalloidin-induced hepatotoxicity as indicated by the lack of elevation in serum levels of ALT (Fig. 6A). Histological analysis showed that after phalloidin treatment, there was extensive hemorrhagic necrosis of the liver characterized by numerous nonfatty vacuoles in wild-type mouse liver (Fig. 6B), whereas Oatp1b2-null mouse liver remained normal (Fig. 6C). In a separate experiment, Oatp1b2-null mice remained active 24 h after being injected ip with 2.5 mg/kg of phalloidin, and there was no elevation of serum levels of ALT or urea nitrogen (data not shown), indicating that there was no delayed hepatotoxicity or injury to kidneys. In contrast, Oatp1b2-null mice were similarly sensitive to α-amanitin–induced hepatotoxicity compared with wild-type mice 16 h after ip injection of α-amanitin (1.0 mg/kg) indicated by similarly elevated serum levels of ALT in 3 groups of mice treated with a-amanitin (Fig. 6A).

Protection of Oatp1b2-null Mice from Microcystin-LR–induced Hepatotoxicity

Three of six C57BL/6 mice died 20 h after ip injection of microcystin-LR (120 μg/kg), whereas all six Oatp1b2-null mice (backcrossed to C57BL/6 for six generations) survived. Microcystin-LR induced severe liver injury in C57BL/6 mice, evident by the markedly elevated serum levels of both ALT and ALP (Fig. 7A), indicating that both hepatocytes and cholangiocytes were injured. In contrast, serum levels of both ALT and ALP remained unchanged in Oatp1b2-null mice (Fig. 7A). Histological analysis showed that after microcystin-LR treatment, there was extensive hemorrhagic necrosis of the liver in wild-type mouse liver (Fig. 7B), whereas Oatp1b2-null mouse liver remained normal (Fig. 7C). Thus, Oatp1b2 is critical in mediating the hepatotoxicity of microcystin-LR. Additionally, there was no acute nephrotoxicity induced by microcystin-LR in either genotype of mice as indicated by a lack of elevation in serum levels of urea nitrogen (data not shown).

After uptake into hepatocytes, microcystin-LR binds tightly to protein phosphatase 1/2a (PP1/2a) in mouse nuclei; the microcystin-PP1/2a adducts (at approximately 40 kDa) can be detected by Western blot (Guzman and Solter, 2002). As shown in Figure 7D, in microcystin-LR treated C57BL/6 mouse liver samples (lanes 1–2), the anti-microcystin antibody detected two strong bands (~40 kDa), which were absent in untreated mouse liver (lane 5). The two ~40-kDa bands were much weaker in Oatp1b2-null mouse livers (lanes 3–4) compared with C57BL/6 mouse livers (lanes 1–2).

DISCUSSION

The present study demonstrates that the first mice null for the liver-specific importer Oatp1b2 have been generated. Oatp1b2-null mice develop normally and breed well. However, Oatp1b2-null mice have moderately altered blood chemistry. Compared with wild-type mice, Oatp1b2-null mice have higher plasma levels and lower biliary excretion of

DBSP after a bolus dose, as well as higher rates of bile flow after administration of phalloidin and $E_2$17βG. Phalloidin and microcystin-LR cause severe hepatotoxicity in wild-type mice but not in Oatp1b2-null mice. However, Oatp1b2-null mice are similarly sensitive as wild-type mice to α-amanitin–induced hepatotoxicity.

Currently, the mechanism of apparent induction of Oatp1a4 in the liver of Oatp1b2-null mice remains unknown. Oatp1a4 is closely linked with Oatp1b2 on chromosome 6. Thus, the disruption of Oatp1b2 gene might result in a compensatory induction of its neighbor gene, Oatp1a4. Previous *in vitro* studies demonstrate that Oatp1a4 transports $E_2$17βG, but not phalloidin or microcystin-LR (Fischer *et al*., 2005; Meier-Abt *et al*., 2004). Thus, the induction of Oatp1a4 in Oatp1b2-null mice may compensate for Oatp1b2 in hepatic uptake of $E_2$17βG and other common substrates for Oatps, but has no effect on hepatic uptake or toxicity of phalloidin or microcystin-LR.

Upon uptake into hepatocytes, the nonmetabolizable organic dye, DBSP is rapidly excreted into bile without biotransformation. Thus, in Oatp1b2-null mice, a slower uptake of DBSP into liver results in a slower rate of biliary excretion of DBSP. Loss of Oatp1b2 will decrease the rate of biliary excretion of its substrates that do not undergo further biotransformation.

The degree of decrease in bile flow by $E_2$17βG has been shown to be dose-dependent in the range of 8.5–21 μmol/kg iv (Meyers *et al*., 1980). Thus, the initial partial protection of the decrease in bile flow in Oatp1b2-null mice (Fig. 4) indicates that hepatic uptake of $E_2$17βG is partially decreased in Oatp1b2-null mice at early time points, which is consistent with the fact that Oatp1a1 and Oatp1a4 also transport $E_2$17βG. The lack of significant difference in bile flow between wild-type and Oatp1b2-null mice at a later time after $E_2$17βG administration (1 h) suggests that Oatp1a1 and Oatp1a4 can compensate with time for Oatp1b2 in hepatic uptake of certain common Oatp substrates under physiological conditions.

The mushroom toxin phalloidin specifically causes hepatotoxicity after parenteral injection, and is only toxic to hepatocytes (Frimmer, 1987). Phalloidin cannot be degraded by peptidases or proteases in animals (Frimmer, 1987). The complete protection of phalloidin-induced hepatotoxicity in Oatp1b2-null mice (Fig. 6) is consistent with phalloidin being a specific substrate for rat Oatp1b2 *in vitro* (Meier-Abt *et al*., 2004). The lack of hepatic uptake of phalloidin in Oatp1b2-null mice is confirmed by the absence of phalloidin-FITC in Oatp1b2-null hepatocytes. The mild decrease in bile flow in Oatp1b2-null mice may be due to a membrane-disturbing effect of phalloidin, which is evident by a transient gastrointestinal discomfort after oral ingestion of phalloidin (Frimmer, 1987).

Oral ingestion of phalloidin is not hepatotoxic due to the inability of intestinal cells to take up phalloidin (Petzinger *et al*., 1982). In contrast, α-amanitin, a cyclic peptide structurally similar to phalloidin, causes liver injury in humans after accidental ingestion of Amanita phalloides (Jaeger *et al*., 1993). Cellular studies indicate that OATP1B1 is the primary transporter for phalloidin, whereas OATP1B3 only weakly transports phalloidin (Fehrenbach *et al*., 2003; Meier-Abt *et al*., 2004). In contrast, α-amanitin is transported by OATP1B3 but not OATP1B1 (Letschert *et al*., 2006), and α-amanitin only weakly inhibits the uptake of phalloidin by OATP1B1 (Fehrenbach *et al*., 2003). Cellular studies indicate that the liver-specific importer rat Ntcp (Gundala *et al*., 2004) and human OATP1B3 (Letschert *et al*. 2006) transport α-amanitin. Thus, Ntcp and OATP1B3 may mediate hepatic uptake of α-amanitin in rodents and humans, respectively.

The present study demonstrates that Oatp1b2 is essential in mediating microcystin-LR–induced hepatotoxicity. After iv administration, the cyclic peptide microcystin-LR is highly

concentrated and accumulates in mouse liver (Robinson *et al*., 1991); the inhibition of serine/threonine PP 1 and 2A by microcystin-LR causes hepatic hemorrhage and necrosis at high doses, and promotes liver cancer at low doses (Gehringer, 2004). The complete protection of Oatp1b2-null mice against microcystin-induced hepatotoxicity is consistent with the *in vitro* results of Oatp1b2 being the sole hepatic importer for microcystin-LR in rodents (Fischer *et al*., 2005). Both OATP1B1 and OATP1B3 can transport microcystin-LR (Fischer *et al*., 2005), and cells expressing OATP1B1/1B3 are highly sensitive to microcystin-LR cytotoxicity compared with wild-type cells (Komatsu *et al*., 2007; Monks *et al*., 2007), demonstrating a critical role of OATP1B1/1B3 in mediating cellular uptake and toxicity of microcystin. Although microcystin-LR is selectively toxic to liver *in vivo* and hepatocytes *in vitro*, exposure of other types of cells to microcystin-LR at higher concentrations for a longer period of time results in cell death (Khan *et al*., 1995). In the present study, the binding of microcystin-LR to PP1/2a was attenuated, but not abolished, in livers of Oatp1b2-null mice, indicating that in addition to Oatp1b2-mediated transport, microcystin-LR can enter cells by passive diffusion or other mechanism(s) at a lower rate. Different from the non-cell-permeable phalloidin, microcystin-LR is bioavailable, and the hepatotoxicity of oral microcystin-LR markedly increases in aged mice, most likely due to increased intestinal absorption (Ito *et al*., 1997). The development of primary liver cancer in China has been linked to a long-term chronic exposure to microcystin as a result of contamination of drinking water (Ueno *et al*., 1996). Thus, the essential role of Oatp1b2 and OATP1B1/1B3 in mediating microcystin-LR hepatotoxicity has important clinical and public health implications.

Currently, the mechanism of a female-selective development of conjugated hyperbilirubinemia in Oatp1b2-null mice is unknown, but the data suggest that Oatp1b2 plays an important role in bilirubin homeostasis. Unconjugated bilirubin produced in splenic macrophages is released into blood, bound to albumin, and distributed to liver, where it is conjugated with glucuronic acid and excreted into bile via Mrp2 (Klaassen and Lu, 2007). Consequently, conjugated bilirubin is difficult to detect in normal mouse blood. Hyperbilirubinemia occurs during cholestasis. However, the female-selective conjugated hyperbilirubinemia is not due to cholestasis, because the rate of bile flow remains unchanged in Oatp1b2-null females compared with wild-type females (Fig. 4). Uridine diphosphate glucuronosyltransferase 1a1 (Ugt1a1), the sole enzyme glucuronidating bilirubin (Kamisako *et al*., 2000), is expressed at higher levels in female than male mouse liver (Buckley and Klaassen, 2007). Hepatic expression of Oatp1a1, which is able to transport bilirubin glucuronide (Kamisako *et al*., 2000), is lower in female than male mice (Cheng *et al*., 2005). In contrast, Mrp3, a basolateral exporter retro-transporting bilirubin glucuronides from liver into blood during cholestasis (Belinsky *et al*., 2005), is expressed at higher levels in females than males (Fig. 2). Bilirubin glucuronides formed within hepatocytes can be excreted into bile via Mrp2, or transported back into blood via Mrp3. *In vitro* studies demonstrate that multiple Oatps (Oatp1a1 and OATP1B1) are capable of transporting bilirubin glucuronides (Cui *et al*., 2001; Kamisako *et al*., 2000). OATP1B1 and OATP1B3 have high affinities for bilirubin glucuronides (K_m at nanomolar concentrations) (Cui *et al*., 2001), suggesting that bilirubin glucuronides pumped out by Mrp3 could be readily taken back into hepatocytes by Oatp1b2. Thus, we speculate that gender differences in hepatic expression of Ugt1a1, Mrp3, and Oatp1a1 may result in a gender difference in hepatic production, efflux, and reuptake of bilirubin glucuronides, leading to a conjugated hyperbilirubinemia selectively in Oatp1b2-null female mice.

In summary, the present study demonstrates a gender-selective development of conjugated hyperbulirubinemia in female Oatp1b2-null mice. Oatp1b2 plays key roles in hepatic uptake and toxicity of phalloidin and microcystin-LR, and is important in determining systemic disposition of DBSP, a model chemical used for liver function assay. Reduction in

OATP1B1 function in populations with functional polymorphisms and/or in pathophysiological conditions is common in humans. Oatp1b2-null mice will be very useful to elucidate how a loss/decrease of Oatp1b2 and OATP1B1/1B3 function disturbs the homeostasis of endogenous chemicals and influences the hepatic uptake and systemic exposure to environmental chemicals and therapeutic drugs.

Acknowledgments

We thank Drs Lauren Aleksunes, Chuan Chen, and Matthew Dieter for technical assistance.

FUNDING National Institutes of Health (ES009649, ES09716, ES013714, and RR021940).

REFERENCES

Belinsky MG, Dawson PA, Shchaveleva I, Bain LJ, Wang R, Ling V, Chen ZS, Grinberg A, Westphal H, Klein-Szanto A, et al. Analysis of the in vivo functions of Mrp3. Mol. Pharmacol. 2005; 68:160–168. [PubMed: 15814571]

Bischoff K. The toxicology of microcystin-LR: Occurrence, toxicokinetics, toxicodynamics, diagnosis and treatment. Vet. Hum. Toxicol. 2001; 43:294–297. [PubMed: 11577938]

Buckley DB, Klaassen CD. Tissue- and gender-specific mRNA expression of UDP-glucuronosyltransferases (UGTs) in mice. Drug Metab. Dispos. 2007; 35:121–127. [PubMed: 17050650]

Buist SC, Klaassen CD. Rat and mouse differences in gender-predominant expression of organic anion transporter (Oat1-3; Slc22a6-8) mRNA levels. Drug Metab. Dispos. 2004; 32:620–625. [PubMed: 15155553]

Canales RD, Luo Y, Willey JC, Austermiller B, Barbacioru CC, Boysen C, Hunkapiller K, Jensen RV, Knight CR, Lee KY, et al. Evaluation of DNA microarray results with quantitative gene expression platforms. Nat. Biotechnol. 2006; 24:1115–1122. [PubMed: 16964225]

Chen C, Slitt AL, Dieter MZ, Tanaka Y, Scheffer GL, Klaassen CD. Up-regulation of Mrp4 expression in kidney of Mrp2-deficient TR- rats. Biochem. Pharmacol. 2005; 70:1088–1095. [PubMed: 16099435]

Cheng X, Maher J, Chen C, Klaassen CD. Tissue distribution and ontogeny of mouse organic anion transporting polypeptides (Oatps). Drug Metab. Dispos. 2005; 33:1062–1073. [PubMed: 15843488]

Choudhuri S, Ogura K, Klaassen CD. Cloning of the full-length coding sequence of rat liver-specific organic anion transporter-1 (rlst-1) and a splice variant and partial characterization of the rat lst-1 gene. Biochem. Biophys. Res. Commun. 2000; 274:79–86. [PubMed: 10903899]

Cui Y, Konig J, Leier I, Buchholz U, Keppler D. Hepatic uptake of bilirubin and its conjugates by the human organic anion transporter SLC21A6. J. Biol. Chem. 2001; 276:9626–9630. [PubMed: 11134001]

Dhumeaux D, Berthelot P, Javitt NB. Dibromsulphalein (DBSP) estimation of hepatic transport function in man. Eur. J. Clin. Invest. 1974; 4:181–185. [PubMed: 4838695]

Eriksson JE, Gronberg L, Nygard S, Slotte JP, Meriluoto JA. Hepatocellular uptake of 3H-dihydromicrocystin-LR, a cyclic peptide toxin. Biochim. Biophys. Acta. 1990; 1025:60–66. [PubMed: 2369577]

Fagan EA. Intrahepatic cholestasis of pregnancy. Clin. Liver Dis. 1999; 3:603–632. [PubMed: 11291241]

Faulstich H, Wieland T. New aspects of amanitin and phalloidin poisoning. Adv. Exp. Med. Biol. 1996; 391:309–314. [PubMed: 8726069]

Fehrenbach T, Cui Y, Faulstich H, Keppler D. Characterization of the transport of the bicyclic peptide phalloidin by human hepatic transport proteins. Naunyn Schmiedebergs Arch. Pharmacol. 2003; 368:415–420. [PubMed: 14530907]

Fischer WJ, Altheimer S, Cattori V, Meier PJ, Dietrich DR, Hagenbuch B. Organic anion transporting polypeptides expressed in liver and brain mediate uptake of microcystin. Toxicol. Appl. Pharmacol. 2005; 203:257–263. [PubMed: 15737679]

Frimmer M. What we have learned from phalloidin. Toxicol. Lett. 1987; 35:169–182. [PubMed: 3824408]

Gehringer MM. Microcystin-LR and okadaic acid-induced cellular effects: A dualistic response. FEBS Lett. 2004; 557:1–8. [PubMed: 14741332]

Gregus Z, Klaassen CD. Comparison of Biliary excretion of organic anions in mice and rats. Toxicol. Appl. Pharmacol. 1982; 63:13–20. [PubMed: 6176049]

Gundala S, Wells LD, Milliano MT, Talkad V, Luxon BA, Neuschwander-Tetri BA. The hepatocellular bile acid transporter Ntcp facilitates uptake of the lethal mushroom toxin alpha-amanitin. Arch. Toxicol. 2004; 78:68–73. [PubMed: 14598021]

Guzman RE, Solter PF. Characterization of sublethal microcystin-LR exposure in mice. Vet. Pathol. 2002; 39:17–26. [PubMed: 12102214]

Hagenbuch B, Adler ID, Schmid TE. Molecular cloning and functional characterization of the mouse organic-anion-transporting polypeptide 1 (Oatp1) and mapping of the gene to chromosome X. Biochem. J. 2000; 345(Pt 1):115–120. [PubMed: 10600646]

Hagenbuch B, Meier PJ. The superfamily of organic anion transporting polypeptides. Biochim. Biophys. Acta. 2003; 1609:1–18. [PubMed: 12507753]

Hagenbuch B, Meier PJ. Organic anion transporting polypeptides of the OATP/SLC21 family: Phylogenetic classification as OATP/SLCO superfamily, new nomenclature and molecular/functional properties. Pflugers Arch. 2004; 447:653–665. [PubMed: 14579113]

Ho RH, Choi L, Lee W, Mayo G, Schwarz UI, Tirona RG, Bailey DG, Stein C. Michael, Kim RB. Effect of drug transporter genotypes on pravastatin disposition in European- and African-American participants. Pharmacogenet. Genomics. 2007; 17:647–656. [PubMed: 17622941]

Ieiri I, Suwannakul S, Maeda K, Uchimaru H, Hashimoto K, Kimura M, Fujino H, Hirano M, Kusuhara H, Irie S, et al. SLCO1B1 (OATP1B1, an uptake transporter) and ABCG2 (BCRP, an efflux transporter) variant alleles and pharmacokinetics of pitavastatin in healthy volunteers. Clin. Pharmacol. Ther. 2007; 82:541–547. [PubMed: 17460607]

Ito E, Kondo F, Harada K. Hepatic necrosis in aged mice by oral administration of microcystin-LR. Toxicon. 1997; 35:231–239. [PubMed: 9080580]

Jaeger A, Jehl F, Flesch F, Sauder P, Kopferschmitt J. Kinetics of amatoxins in human poisoning: Therapeutic implications. J. Toxicol. Clin. Toxicol. 1993; 31:63–80. [PubMed: 8433416]

Kamisako T, Kobayashi Y, Takeuchi K, Ishihara T, Higuchi K, Tanaka Y, Gabazza EC, Adachi Y. Recent advances in bilirubin metabolism research: The molecular mechanism of hepatocyte bilirubin transport and its clinical relevance. J. Gastroenterol. 2000; 35:659–664. [PubMed: 11023036]

Khan SA, Ghosh S, Wickstrom M, Miller LA, Hess R, Haschek WM, Beasley VR. Comparative pathology of microcystin-LR in cultured hepatocytes, fibroblasts, and renal epithelial cells. Nat. Toxins. 1995; 3:119–128. [PubMed: 7648020]

Klaassen CD, Lu H. Xenobiotic transporters: Ascribing function from gene knockout and mutation studies. Toxicol. Sci. 2008; 101:186–196. [PubMed: 17698509]

Komatsu M, Furukawa T, Ikeda R, Takumi S, Nong Q, Aoyama K, Akiyama S, Keppler D, Takeuchi T. Involvement of mitogen-activated protein kinase signaling pathways in microcystin-LR-induced apoptosis after its selective uptake mediated by OATP1B1 and OATP1B3. Toxicol. Sci. 2007; 97:407–416. [PubMed: 17369605]

Konig J, Seithel A, Gradhand U, Fromm MF. Pharmacogenomics of human OATP transporters. Naunyn Schmiedebergs Arch. Pharmacol. 2006; 372:432–443. [PubMed: 16525793]

Kroncke KD, Fricker G, Meier PJ, Gerok W, Wieland T, Kurz G. alpha-Amanitin uptake into hepatocytes. Identification of hepatic membrane transport systems used by amatoxins. J. Biol. Chem. 1986; 261:12562–12567. [PubMed: 3745203]

Leazer TM, Klaassen CD. The presence of xenobiotic transporters in rat placenta. Drug Metab. Dispos. 2003; 31:153–167. [PubMed: 12527696]

Letschert K, Faulstich H, Keller D, Keppler D. Molecular characterization and inhibition of amanitin uptake into human hepatocytes. Toxicol. Sci. 2006; 91:140–149. [PubMed: 16495352]

Li N, Hartley DP, Cherrington NJ, Klaassen CD. Tissue expression, ontogeny, and inducibility of rat organic anion transporting polypeptide 4. J. Pharmacol. Exp. Ther. 2002; 301:551–560. [PubMed: 11961056]

Maher JM, Slitt AL, Cherrington NJ, Cheng X, Klaassen CD. Tissue distribution and hepatic and renal ontogeny of the multidrug resistance-associated protein (Mrp) family in mice. Drug Metab. Dispos. 2005; 33:947–955. [PubMed: 15802388]

Meier-Abt F, Faulstich H, Hagenbuch B. Identification of phalloidin uptake systems of rat and human liver. Biochim. Biophys. Acta. 2004; 1664:64–69. [PubMed: 15238259]

Meyers M, Slikker W, Pascoe G, Vore M. Characterization of cholestasis induced by estradiol-17 beta-D-glucuronide in the rat. J. Pharmacol. Exp. Ther. 1980; 214:87–93. [PubMed: 7391975]

Monks NR, Liu S, Xu Y, Yu H, Bendelow AS, Moscow JA. Potent cytotoxicity of the phosphatase inhibitor microcystin LR and microcystin analogues in OATP1B1- and OATP1B3-expressing HeLa cells. Mol. Cancer Ther. 2007; 6:587–598. [PubMed: 17308056]

Niemi M, Backman JT, Kajosaari LI, Leathart JB, Neuvonen M, Daly AK, Eichelbaum M, Kivisto KT, Neuvonen PJ. Polymorphic organic anion transporting polypeptide 1B1 is a major determinant of repaglinide pharmacokinetics. Clin. Pharmacol. Ther. 2005a; 77:468–478. [PubMed: 15961978]

Niemi M, Kivisto KT, Hofmann U, Schwab M, Eichelbaum M, Fromm MF. Fexofenadine pharmacokinetics are associated with a polymorphism of the SLCO1B1 gene (encoding OATP1B1). Br. J. Clin. Pharmacol. 2005b; 59:602–604. [PubMed: 15842561]

Ogura K, Choudhuri S, Klaassen CD. Full-length cDNA cloning and genomic organization of the mouse liver-specific organic anion transporter-1 (lst-1). Biochem. Biophys. Res. Commun. 2000; 272:563–570. [PubMed: 10833452]

Pasanen MK, Neuvonen M, Neuvonen PJ, Niemi M. SLCO1B1 polymorphism markedly affects the pharmacokinetics of simvastatin acid. Pharmacogenet. Genomics. 2006; 16:873–879. [PubMed: 17108811]

Petzinger E, Burckhardt G, Schwenk M, Faulstich H. Lack of intestinal transport of [3H]-demethylphalloin: Comparative studies with phallotoxins and bile acids on isolated small intestinal cells and ileal brush border membrane vesicles. Naunyn Schmiedebergs Arch. Pharmacol. 1982; 320:196–200. [PubMed: 7121618]

Robinson NA, Pace JG, Matson CF, Miura GA, Lawrence WB. Tissue distribution, excretion and hepatic biotransformation of microcystin-LR in mice. J. Pharmacol. Exp. Ther. 1991; 256:176–182. [PubMed: 1988656]

Trauner M, Boyer JL. Bile salt transporters: Molecular characterization, function, and regulation. Physiol. Rev. 2003; 83:633–671. [PubMed: 12663868]

Ueno Y, Nagata S, Tsutsumi T, Hasegawa A, Watanabe MF, Park HD, Chen GC, Chen G, Yu SZ. Detection of microcystins, a blue-green algal hepatotoxin, in drinking water sampled in Haimen and Fusui, endemic areas of primary liver cancer in China, by highly sensitive immunoassay. Carcinogenesis. 1996; 17:1317–1321. [PubMed: 8681449]

Zhang W, He YJ, Han CT, Liu ZQ, Li Q, Fan L, Tan ZR, Zhang WX, Yu BN, Wang D, et al. Effect of SLCO1B1 genetic polymorphism on the pharmacokinetics of nateglinide. Br. J. Clin. Pharmacol. 2006; 62:567–572. [PubMed: 16796707]

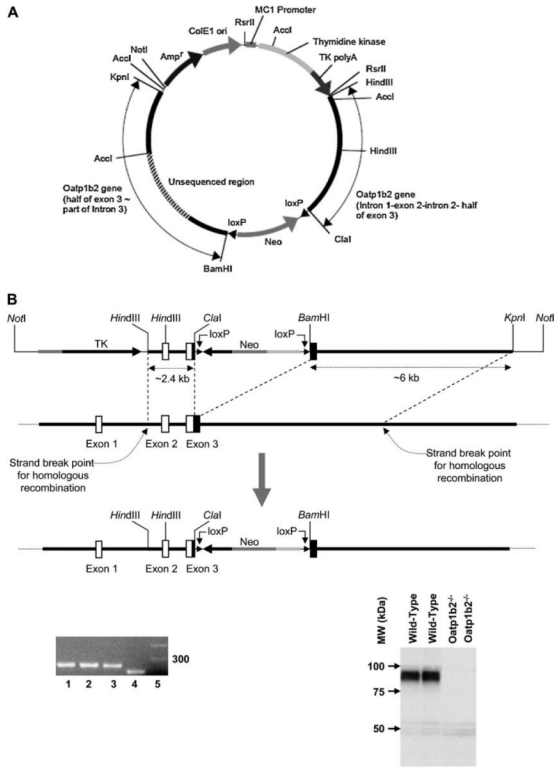

FIG. 1.

Generation and identification of Oatp1b2-null mice. (A) Schematic structure of targeting vector. (B) Upper panel, targeting strategy through homologous recombination; Lower panel, left: PCR genotyping of Oatp1b2-null and wild-type mice. Lanes 1–3, Oatp1b2-null; lane 4, wild-type; lane 5, 100 bp DNA ladder. Lower panel, right: Western blot detection of protein expression of Oatp1b2 in liver of wild-type and Oatp1b2-null mice.

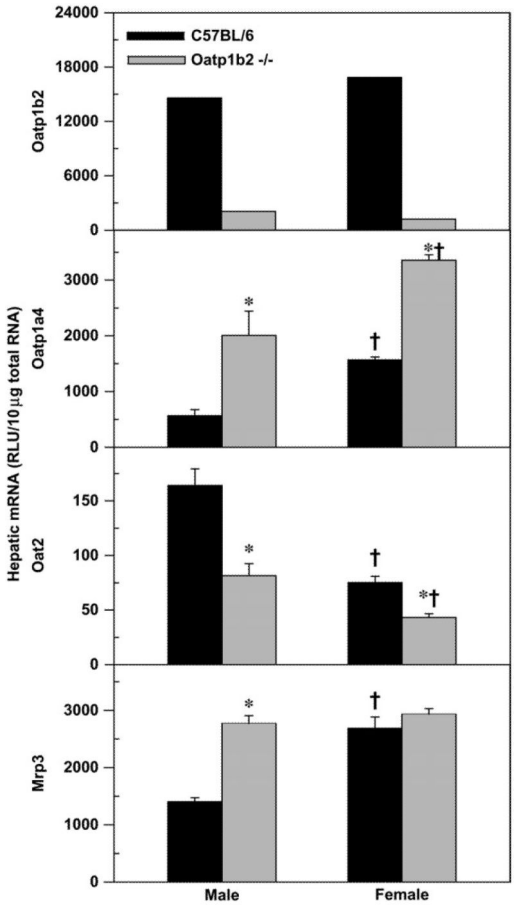

FIG. 2.

mRNA expression of transporters in livers of adult (3 months old) male and female C57BL/6 and Oatp1b2-null mice. Tissue mRNA expression of Oatp1b2, Oatp1a4, Oat2, and Mrp3 was determined with the branched DNA signal amplification assay. Data are presented as mean ± standard error of six livers except that pooled RNA samples from six livers were used to determine Oatp1b2 mRNA. *$p < 0.05$ compared with the same gender C57BL/6 group. †$p < 0.05$ compared with male C57BL/6 group.

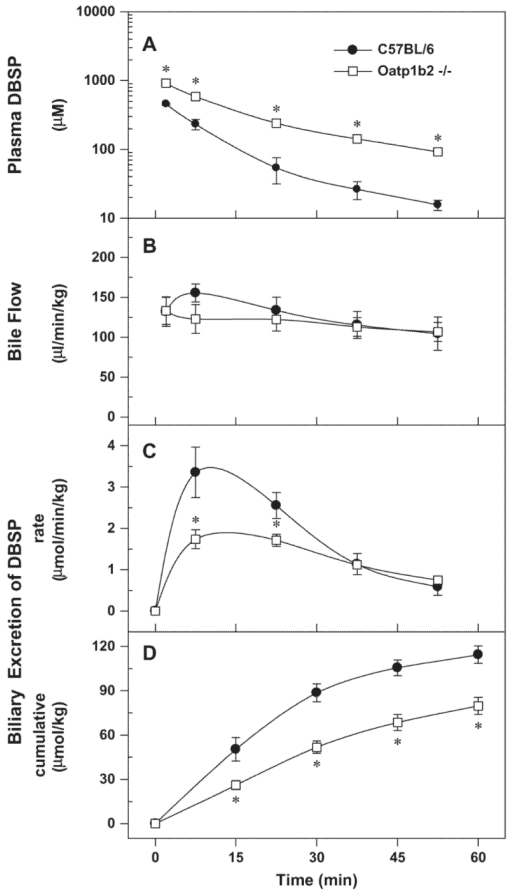

FIG. 3.

Plasma levels (A), bile flow (B), and biliary excretion (C, D) of DBSP in male C57BL/6 and Oatp1b2-null mice. Mice were administered a bolus intra-arterial dose of DBSP (120 μmol/kg). Data are presented as mean ± standard error of four to five samples. *$p < 0.05$ compared with C57BL/6 group.

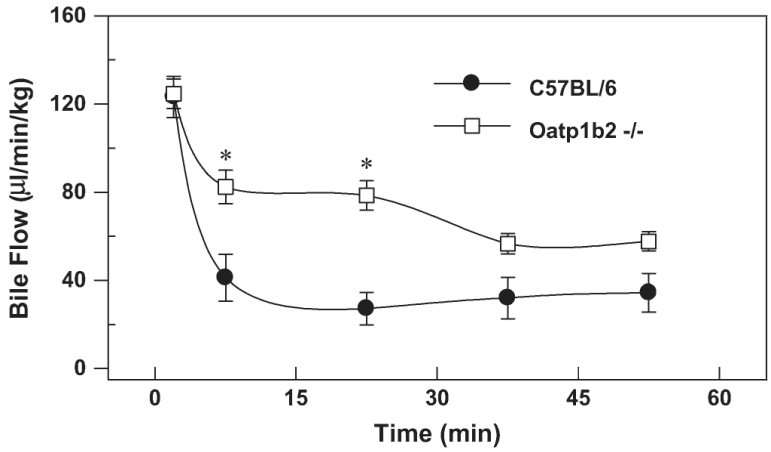

FIG. 4.

Partial protection of Oatp1b2-null mice from estradiol-17β-D-glucuronide ($E_2$17βG)-induced decrease in bile flow. Female adult C57BL/6 and Oatp1b2-null mice were administered a bolus intra-arterial dose of $E_2$17βG (24 μmol/kg). Data are presented as mean ± standard error of four to five samples. *$p < 0.05$ compared with C57BL/6 group.

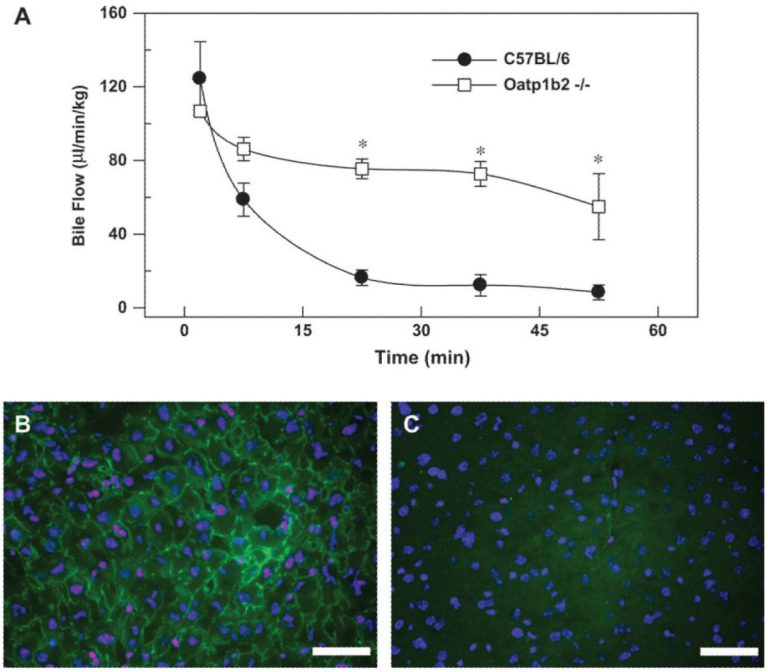

FIG. 5.

Protection of Oatp1b2-null mice from phalloidin-induced cholestasis. Male adult C57BL/6 and Oatp1b2-null mice were administered a bolus intra-arterial dose of phalloidin 400 μg/kg (320 μg/kg phalloidin + 80 μg/kg phalloidin-FITC). (A) Bile flow in C57BL/6 and Oatp1b2-null mice after phalloidin administration. Data are presented as mean ± standard error of four to five samples. *$p < 0.05$ compared with C57BL/6 group. Hepatic uptake of phalloidin-FITC in C57BL/6 (B) and Oatp1b2-null mice (C) 1 h after intra-arterial administration of phalloidin. Phalloidin-FITC (in green) bound to the inner membrane of hepatocytes in wild-type mouse liver. The nuclei (in blue) were stained with DAPI. Bar = 50 μm.

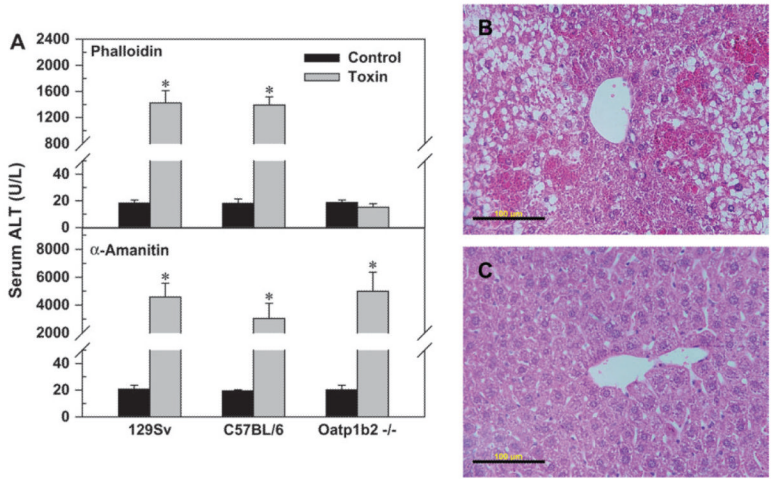

FIG. 6.

Differential roles of Oatp1b2 in hepatotoxicity induced by phalloidin and a-amanitin. Male adult 129Sv, C57BL/6, and Oatp1b2-null (in a mixed background of 129Sv and C57BL/6) mice were injected ip with phalloidin (2.5 mg/kg in saline), α-amanitin (1.0 mg/kg in saline), or an equal volume of saline (10 ml/kg) as vehicle control. Blood and liver samples were collected 6-h (phalloidin) or 16-h (α-amanitin) postinjection for analyzing serum levels of ALT and examining liver histopathology. (A) Serum levels of ALT in wild-type and Oatp1b2-null mice administered phalloidin and α-amanitin. Data are presented as mean ± standard error of five to nine samples. *$p < 0.05$ compared with vehicle control. Histopathology of phalloidin-treated wild-type (B) and Oatp1b2-null (C) mouse livers. Liver sections (5 μm) were stained with hematoxylin–eosin. Bar = 100 μm.

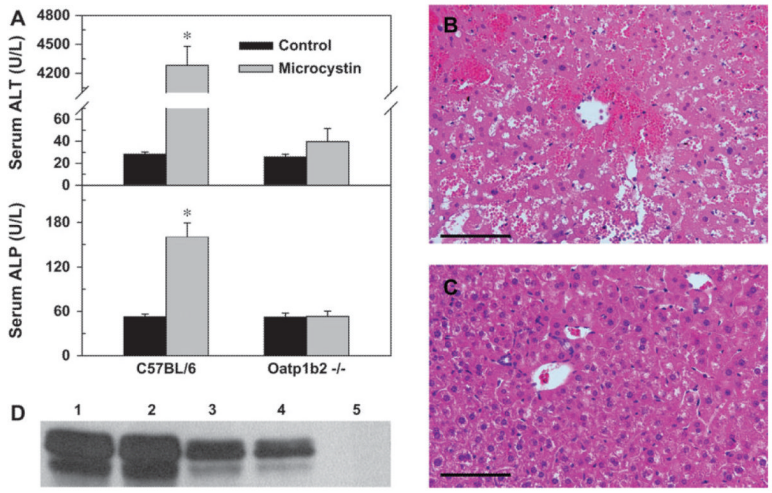

FIG. 7.

(A) Serum levels of ALT and ALP in C57BL/6 and Oatp1b2-null mice treated with microcystin-LR. Male adult wild-type (C57BL/6) and Oatp1b2-null (in C57BL/6 background) mice were injected ip with microcystin-LR (120 μg/kg in saline) or an equal volume of saline (10 ml/kg) as vehicle control. Blood and liver samples were collected 20-h postinjection for analyzing serum levels of ALT and ALP as well as examining liver histopathology. Data are presented as mean ± standard error of three to six samples. *$p <$ 0.05 compared with vehicle control. Histopathology of microcystin-LR–treated wild-type (B) and Oatp1b2-null (C) mouse livers. Liver sections (5 μm) were stained with hematoxylin–eosin. Bar = 100 μm. (D) Western blot detection of binding of microcystin-LR to PP 1 and 2a in nuclear or cytosolic proteins prepared from mouse livers 3 h after ip injection of microcystin-LR (60 μg/kg). Lanes 1–2, C57BL/6 mouse livers treated with microcystin-LR; lanes 3–4, Oatp1b2-null mouse livers treated with microcystin-LR; lane 5, untreated mouse liver.

TABLE 1

Blood Chemistry in C57BL/6 and Oatp1b2 Knockout (Oatp1b2-null) Mice

	C57BL/6 male	Oatp1b2-null male	C57BL/6 female	Oatp1b2-null female
Total protein (g/dl)	3.93 ± 0.07	4.25 ± 0.10*	3.78 ± 0.04	3.98 ± 0.07†
Albumin (g/dl)	2.37 ± 0.05	2.60 ± 0.05*	2.30 ± 0.02	2.43 ± 0.04†
Bilirubin total (mg/dl)	0.12 ± 0.02	0.18 ± 0.02	0.10 ± 0.00	0.35 ± 0.05†
Bilirubin conjugated (mg/dl)	0.0 ± 0.0	0.020 ± 0.016	0.0 ± 0.0	0.22 ± 0.04†
Bilirubin unconjugated (mg/dl)	0.12 ± 0.02	0.18 ± 0.02	0.10 ± 0.0	0.13 ± 0.02
ALT (U/l)	23 ± 2.3	22 ± 1.3	14 ± 0.5	17 ± 1.2†
Sodium (mEq/l)	147 ± 0.9	148 ± 0.5	145 ± 0.6	148 ± 0.6†
Chloride (mEq/l)	119 ± 0.9	120 ± 0.8	117 ± 0.6	119 ± 0.6†
Amylase (U/l)	1817 ± 88	1854 ± 128	1337 ± 43	1200 ± 33†
Cholesterol (mg/dl)	60 ± 2	78 ± 3*	53 ± 2	60 ± 3

Note. $N = 6$. Mean ± standard error.

*$p < 0.05$ compared with male wild-type,

†$p < 0.05$ compared with female wild-type mice. Adult age-matched (3 months old) male and female C57BL/6 mice and Oatp1b2-null mice that have been backcrossed to C57BL/6 for six generations were used in this study.

Toxicol Sci. Author manuscript; available in PMC 2011 September 27.